

Lawrence Berkeley National Laboratory

Recent Work

Title

HELIUM PHOTOELECTRON SATELLITES: LOW-ENERGY BEHAVIOR OF THE $n=3-5$ LINES

Permalink

<https://escholarship.org/uc/item/1fk0k0jr>

Author

Lindle, D.W.

Publication Date

1986-08-01

e.2



Lawrence Berkeley Laboratory

UNIVERSITY OF CALIFORNIA

LAWRENCE
BERKELEY LABORATORY

OCT 2 1986

Materials & Molecular Research Division

LIBRARY AND
DOCUMENTS SECTION

Submitted to Physical Review A

HELIUM PHOTOELECTRON SATELLITES: LOW-ENERGY
BEHAVIOR OF THE $n=3-5$ LINES

D.W. Lindle, P.A. Heimann, T.A. Ferrett, and
D.A. Shirley

August 1986

TWO-WEEK LOAN COPY

*This is a Library Circulating Copy
which may be borrowed for two weeks*



LBL-21651

e.2

DISCLAIMER

This document was prepared as an account of work sponsored by the United States Government. While this document is believed to contain correct information, neither the United States Government nor any agency thereof, nor the Regents of the University of California, nor any of their employees, makes any warranty, express or implied, or assumes any legal responsibility for the accuracy, completeness, or usefulness of any information, apparatus, product, or process disclosed, or represents that its use would not infringe privately owned rights. Reference herein to any specific commercial product, process, or service by its trade name, trademark, manufacturer, or otherwise, does not necessarily constitute or imply its endorsement, recommendation, or favoring by the United States Government or any agency thereof, or the Regents of the University of California. The views and opinions of authors expressed herein do not necessarily state or reflect those of the United States Government or any agency thereof or the Regents of the University of California.

Helium Photoelectron Satellites:
Low-Energy Behavior of the $n=3-5$ Lines

D.W. Lindle, P.A. Heimann, T.A. Ferrett, and D.A. Shirley

Materials and Molecular Research Division
Lawrence Berkeley Laboratory
and
Department of Chemistry
University of California
Berkeley, California 94720

Photoelectron satellite branching ratios and asymmetry parameters have been measured for photoionization of atomic He to $\text{He}^+(n)$, where $n=3-5$, at a few photon energies near the satellite thresholds. The $n=3$ and $n=4$ satellite branching ratios relative to the $n=1$ main-line cross section exhibit behavior similar to that previously observed for the $\text{He}^+(n=2)$ satellite. The asymmetry parameter β shows progressively more negative values as n increases, supporting a prediction by Greene for the threshold behavior of the He satellites.

Multi-electron processes in photoionization are affected strongly by electron correlation.¹ Among the manifestations of electron correlation are photoelectron satellites,² which are final ionic states that correspond heuristically to the ionization of one electron and the excitation of a second electron to a higher-lying bound orbital. The most-studied and best-understood satellite, both experimentally³⁻¹³ and theoretically,¹⁴⁻²² is $\text{He}^+(n=2)$, reached by ionization of the $\text{He}(1s^2)$ ground state. This satellite has roughly 10% of the $\text{He}^+(1s)$ main-line intensity near threshold^{4,6,8,9,13} and is composed of the effectively degenerate 2s and 2p final ionic states, which are split only by the Lamb shift. One important finding about electron correlation resulting from the $\text{He}^+(n=2)$ studies has by now been well-documented;^{13,20} close to threshold, electron-electron interactions in the final state [usually called continuum-state configuration interaction (CSCI) or close-coupling] strongly enhance the production of $\text{He}^+(2p)$ relative to $\text{He}^+(2s)$ and $\text{He}^+(1s)$. Experimentally, this enhancement results in a higher satellite-to-main line branching ratio,^{6,8,9,13} and a lower value for the satellite asymmetry parameter.^{9,11-13} Theoretically,¹⁷⁻²¹ proper treatment of the continuum-state interactions has led to a better understanding of this classic example of multi-electron phenomena in He, the simplest atom for which electron correlation is possible.

In contrast to the $\text{He}^+(n=2)$ satellite, less is known about the He satellites with higher values of the principal quantum number, n . The only available results are for $n=3$, for which the satellite cross section has been measured^{13,23} at several photon energies above 80

eV. For the series of $n \geq 3$ satellites, Greene has predicted²⁴ that the asymmetry parameters at threshold will decrease with increasing n , reaching the lower limit for β of -1 as n gets very large. These predictions recently have been confirmed very close to threshold.²⁵ At higher energies, and for higher n , no further work on the He satellites is available. We report here measurements of satellite branching ratios and angular distributions for the $n=3-5$ He satellites in the 76-95 eV photon-energy range.

The experiment was performed at the Stanford Synchrotron Radiation Laboratory, with the same apparatus²⁶ and experimental conditions as in our earlier work on the He+($n=2$) satellite,¹³ with one exception. In the present work on the low-cross-section high- n He satellites, we enhanced the incident photon flux by accepting a poorer photon-energy resolution of 1.3\AA (0.6-1.0 eV in the 76-95 eV range) full-width at half-maximum. Even with this increase in flux over the previous measurements, we still encountered count rates as low as 0.1 sec^{-1} .

The atomic differential photoionization cross section can be described by the expression,²⁷

$$\frac{d\sigma(\theta, h\nu)}{d\Omega} = \frac{\sigma(h\nu)}{4\pi} [1 + \beta(h\nu) P_2(\cos \theta)] , \quad (1)$$

where $\sigma(h\nu)$ and $\beta(h\nu)$ are the partial cross section and the angular-distribution asymmetry parameter of the photoionization process, $P_2(\cos \theta)$ is the second Legendre polynomial, and θ is the angle between the polarization of the incident radiation and the direction of photoelectron emission. Satellite-to-main line branching ratios

were obtained with a single time-of-flight (TOF) electron analyzer placed at the magic angle ($\theta=54.7^\circ$), thereby eliminating any angular dependence of the photoelectron peak intensities. With a second TOF analyzer at $\theta=0^\circ$, we were able to determine the β parameters for the satellites as well. Calibration of the relative satellite peak intensities was accomplished by measuring the known cross sections and asymmetry parameters for Ne 2s and 2p photoelectrons.²⁸

A TOF photoelectron spectrum of He at 80 eV photon energy and with $\theta=54.7^\circ$ is shown in Fig. 1. All of the available He+(n) final states up to n=5 are visible in this spectrum. Their binding energies with increasing n are 24.6, 65.4, 72.9, 75.6, and 76.8 eV, respectively.²⁹ Higher-n satellites and electrons from double ionization (threshold at 79.0 eV) are either too weak or of too low kinetic energy to be observed in this spectrum.

Measured He photoelectron satellite branching ratios relative to the 1s main line, satellite cross sections, and satellite asymmetry parameters are set out in Table I and plotted in Fig. 2. The errors reported for the present data reflect statistical uncertainties only. Systematic errors are harder to estimate, but from previous experience and from comparison of our He+(n=2) results to other workers' measurements, we believe that they are no larger than $\pm 10\%$ for the branching ratios and ± 0.1 for the asymmetry parameters.

The present branching-ratio data were converted to satellite cross sections by multiplying the branching ratios by the 1s partial cross section at each photon energy. The 1s cross sections, in turn, were determined from the known total photoionization cross section of

He³⁰ after consideration of all possible contributions to the total cross section, as follows. The n=2 satellite branching ratios were determined from our TOF spectra and from previous results^{6,8,9,13} to vary between 8-10% in this photon-energy range. For the higher-n satellites, branching ratios were taken from the TOF spectra where possible. At energies for which the higher-n satellites were not measured, we estimated their branching ratios from a threshold determination²⁵ of their intensities relative to the n=2 satellite cross section. At threshold, the $n \geq 3$ satellites contribute approximately 30% of the threshold value for the n=2 cross section.²⁵ Finally, the relative double-ionization cross sections above 79.0 eV were determined from ion-yield measurements.³¹ The n=1 main-line cross section thus was found to lie between 88% and 90% of the total cross section in the 76-95 eV photon-energy range.

Table I and Fig. 2 also include previous measurements^{5,13,23} of the n=3 satellite branching ratio, partial cross section, and asymmetry parameter. The earlier n=3 branching ratios^{5,13} were converted to cross-section values (and vice versa for the previous cross-section measurements²³) using the n=1 main-line cross sections determined as described above. Agreement is good among all of the available data. Recent threshold-electron measurements²⁵ also agree well with the present branching-ratio and angular-distribution results.

The experimental results can be compared to two calculations for the n=3 satellite. Brown¹⁵ predicted a branching ratio of 1.1% at 80 eV. Richards and Larkins^{19,21} used Hartree-Fock calculations to

predict a photon-energy dependence of the $n=3$ cross section in good agreement with the results in Table I.

The $n=3$ and $n=4$ satellite branching ratios are relatively constant at low energy, but both decrease above 90 eV. The magnitude of the decrease for both satellites is 20-40% over the first 20 eV above threshold. A quantitatively similar behavior has been observed for the $n=2$ satellite,^{6,8,9,13} where the branching-ratio decrease is ascribed to a rapid drop in the 2p cross section right above threshold.^{13,17,19-21} This rapid decrease in the 2p cross section has been observed directly in a fluorescence measurement.¹⁰ It has been described as a result of the strong photon-energy dependence of CSCI,^{13,20} to which a considerable fraction of the $\text{He}+(2p)$ intensity can be attributed. Similarly, for the $n=3,4$ satellites, the decrease of their branching ratios with energy may be due to the low-energy importance of final states with angular momenta greater than zero (e.g. 3p and 3d). As the photon energy increases, the continuum-state effects which enhance the higher- ℓ states would diminish, and the branching ratios relative to the 1s cross section would drop. Hartree-Fock calculations¹⁹ indicate that the 3p cross section is enhanced relative to the 3s cross section near threshold.

The $n=3$ branching ratio at 95 eV photon energy also can be compared to the Al $K\alpha$ measurement⁵ of the high-energy limit. To within the poor precision of the high-photon-energy measurements, the results suggest that by 95 eV, the $n=3$ satellite branching ratio already has reached its sudden limit. This would be surprising

because 95 eV is only 22 eV above the satellite threshold, whereas the satellite excitation energy (above the 1s threshold) is 48 eV.

Furthermore, in comparison to the higher-precision $n=2$ branching-ratio results,^{8,9,13} the $n=2$ satellite does not reach its asymptotic value until well above 100 eV photon energy.

Turning now to the asymmetry-parameter results, and comparing the lowest kinetic-energy measurement for each satellite $n=3-5$, we observe that the asymmetry parameter varies from -0.2 to -0.4 to -0.7 with increasing n . This trend has been predicted,²⁴ and in fact the calculations for the threshold behavior of the asymmetry parameters show reasonable quantitative agreement with our results 3-4 eV above threshold. The decrease of the satellite asymmetry parameters at higher n signifies the approach of the multi-electron ionization process to that of complete double ionization, in which the direction of the two outgoing electrons would be highly correlated. Recent work at energies closer to threshold (≤ 1 eV kinetic energy) has found a quantitatively similar result.²⁵

The $n=3,4$ asymmetry parameters exhibit a rapid increase with energy. This behavior results from two effects. First, the populations of the different angular-momentum states making up each satellite may vary as a function of photon energy, and second, the asymmetry parameters for each ℓ state (except $\ell=0$) also may vary with energy. Nevertheless, comparison to the $n=2$ asymmetry-parameter measurements^{9,11-13} suggests that the 3p and 3d, and the 4p, 4d, and 4f final states are relatively more important near threshold.

Greene³² has calculated the ℓ populations of the He satellites at threshold. For $n=3,4$, all available angular-momentum states (i.e. $\ell \leq n$) contribute, with the $\ell=1,2$ states being strongest. Therefore, the faster intensity decrease with energy of the $\ell \geq 1$ final states relative to 3s or 4s, respectively, can in part explain the rapid observed increase in the satellite asymmetry parameters.

In conclusion, we have presented new results on the He+($n=3-5$) photoelectron satellites. Overall, we observe very similar behavior to that exhibited in the case of the He+($n=2$) satellite, suggesting that the effects due to electron correlation seen for $n=2$ also govern the behavior of the higher- n satellites. The asymmetry-parameter results tend to confirm the threshold prediction by Greene²⁴ that the satellite asymmetry parameters approach -1 as n increases. Finally, we hope that this preliminary study to elucidate the trends in the He satellite series will stimulate further experimental and theoretical work to understand the detailed electron-electron interactions which lead to these final states in photoemission.

Acknowledgements

This work was supported by the Director, Office of Energy Research, Office of Basic Energy Sciences, Chemical Sciences Division of the U.S. Department of Energy under Contract No. DE-AC03-76SF00098. It was performed at the Stanford Synchrotron Radiation Laboratory, which is supported by the Department of Energy's Office of Basic Energy Sciences.

References

1. F.J. Wuilleumier in Atomic Physics, vol. 7, edited by D. Kleppner and F.M. Pipkin (Plenum, New York, 1981); Ann. Phys. 4, 231 (1982).
2. S.T. Manson, J. Electron Spectrosc. 9, 21 (1976).
3. T.A. Carlson, Phys. Rev. 156, 142 (1967).
4. J.A.R. Samson, Phys. Rev. Lett. 22, 693 (1969).
5. T.A. Carlson, M.O. Krause, and W.E. Moddeman, J. Phys (Paris) Colloq. 32, C4-76 (1971).
6. M.O. Krause and F. Wuilleumier, J. Phys. B 5, L143 (1972).
7. P.R. Woodruff and J.A.R. Samson, Phys. Rev. Lett. 45, 110 (1980).
8. F. Wuilleumier, M.Y. Adam, N. Sandner, and V. Schmidt, J. Phys. (Paris) Lett. 41, L373 (1980).
9. J.M. Bizau, F. Wuilleumier, P. Dhez, D.L. Ederer, T.N. Chang, S. Krummacher, and V. Schmidt, Phys. Rev. Lett. 48, 588 (1982).
10. P.R. Woodruff and J.A.R. Samson, Phys. Rev. A 25, 848 (1982).
11. V. Schmidt, H. Derenbach, and R. Malutzki, J. Phys. B 15, L523 (1982).
12. P. Morin, M.Y. Adam, I. Nenner, J. Delwiche, M.J. Hubin-Franskin, and P. Lablanquie, Nucl. Instrum. Methods 208, 761 (1983).
13. D.W. Lindle, T.A. Ferrett, U. Becker, P.H. Kobrin, C.M. Truesdale, H.G. Kerkhoff, and D.A. Shirley, Phys. Rev. A 31, 714 (1985).
14. E.E. Salpeter and M.H. Zaidi, Phys. Rev. 125, 248 (1962).
15. R.L. Brown, Phys. Rev. A 1, 341 (1970).
16. V. Jacobs, Phys. Rev. A 3, 289 (1971).
17. V.L. Jacobs and P.G. Burke, J. Phys. B 5, L67 (1972).
18. T.N. Chang, J. Phys. B 13, L551 (1980).

19. J.A. Richards, Honours Thesis, Monash University, Australia, 1981.
20. K.A Berrington, P.G. Burke, W.C. Fon, and K.T. Taylor, J. Phys. B 15, L603 (1982); see P.C. Ojha, ibid 17, 1807 (1984) for additional discussion.
21. J.A. Richards and F.P. Larkins, J. Electron Spectrosc. 32, 193 (1983).
22. S. Salomonson, S.L. Carter, and H.P. Kelly, J. Phys. B 18, L149 (1985).
23. J.M. Bizau, F.J. Wuilleumier, D.L. Ederer, P. Dhez, S. Krummacher, and V. Schmidt (unpublished).
24. C.H. Greene, Phys. Rev. Lett. 44, 869 (1980).
25. P.A. Heimann, U. Becker, H.G. Kerckhoff, B. Langer, D. Szostak, R. Wehlitz, D.W. Lindle, T.A. Ferrett, and D.A. Shirley (unpublished).
26. M.G. White, R.A. Rosenberg, G. Gabor, E.D. Poliakoff, G. Thornton, S.H. Southworth, and D.A. Shirley, Rev. Sci. Instrum. 50, 1268 (1979).
27. C.N. Yang, Phys. Rev. 74, 764 (1948).
28. F. Wuilleumier and M.O. Krause, J. Electron Spectrosc. 15, 15 (1979).
29. $E_n = E(\text{He}^{++}) - R(Z^2/n^2)$, where E_n is the binding energy of the $\text{He}^+(n)$ satellite, $E(\text{He}^{++})$ is the double-ionization threshold (79.0 eV), and R is the Rydberg (13.6 eV).
30. G.V. Marr and J.B. West, At. Data Nucl. Data Tables 18, 497 (1976).
31. D.M.P. Holland, K. Codling, J.B. West, and G.V. Marr, J. Phys. B 12, 2465 (1979).
32. C.H. Greene (private communication).

Table I: Branching ratios relative to the 1s main line, partial cross sections, and angular-distribution asymmetry parameters for the He+(n=3-5) photoelectron satellites at selected photon energies. Statistical errors are given in the last digit(s) parenthetically.

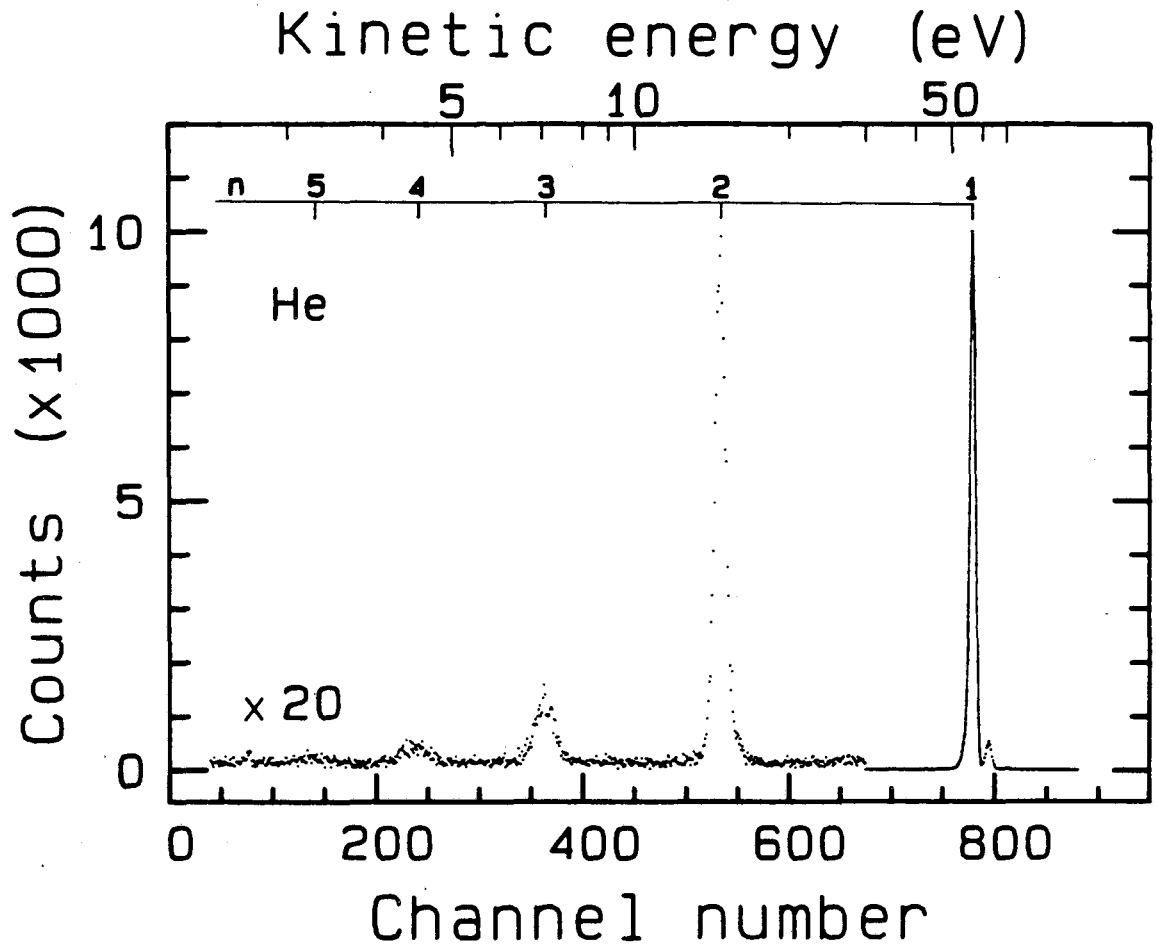
Photon Energy (ev)	Kinetic Energy (eV)	Branching Ratio (%)	Cross Section (Kb) ^a	Asymmetry Parameter (β)
<u>n=3</u>				
72.9 (Ref. 25)	0.0	1.99(7)	15.9(5)	
73.5 (Ref. 25)	0.6			-0.30(16)
74.0 (Ref. 25)	1.1			-0.43(17)
76.0	3.1	1.76(9)	13.0(7)	-0.20(6)
78.0	5.1	1.64(7)	11.4(5)	-0.14(6)
80.0	7.1	1.73(6)	11.4(4)	-0.03(6)
80.0 (Ref. 13)	7.1	1.8(2)	11.8(13)	-0.2(2)
85.0 (Ref. 23)	12.1	1.7(2)	10.0(10)	
86.0	13.1	1.66(5)	9.3(3)	0.16(6)
90.0 (Ref. 23)	17.1	1.5(2)	7.5(10)	
95.0	22.1	1.33(4)	5.9(2)	0.71(7)
95.0 (Ref. 23)	22.1	1.3(2)	6.0(10)	
100.0 (Ref. 23)	27.1	1.3(2)	5.0(7)	
Al K α (Ref. 5)		1.4(8)	0.002(1)	
<u>n=4</u>				
75.6 (Ref. 25)	0.0	1.08(3)	8.0(2)	
76.2 (Ref. 25)	0.6			-0.41(16)
76.7 (Ref. 25)	1.1			-0.45(17)
80.0	4.4	0.67(5)	4.4(3)	-0.39(11)
86.0	10.4	0.70(4)	3.9(2)	-0.09(9)
95.0	19.4	0.42(3)	1.9(1)	0.63(15)
<u>n=5</u>				
76.8 (Ref. 25)	0.0	0.31(2)	2.2(1)	
77.4 (Ref. 25)	0.6			-0.46(17)
77.9 (Ref. 25)	1.1			-0.36(23)
80.0	3.2	0.37(6)	2.4(4)	-0.67(16)

^a1 Kb = 10⁻²¹ cm²

Figure Captions

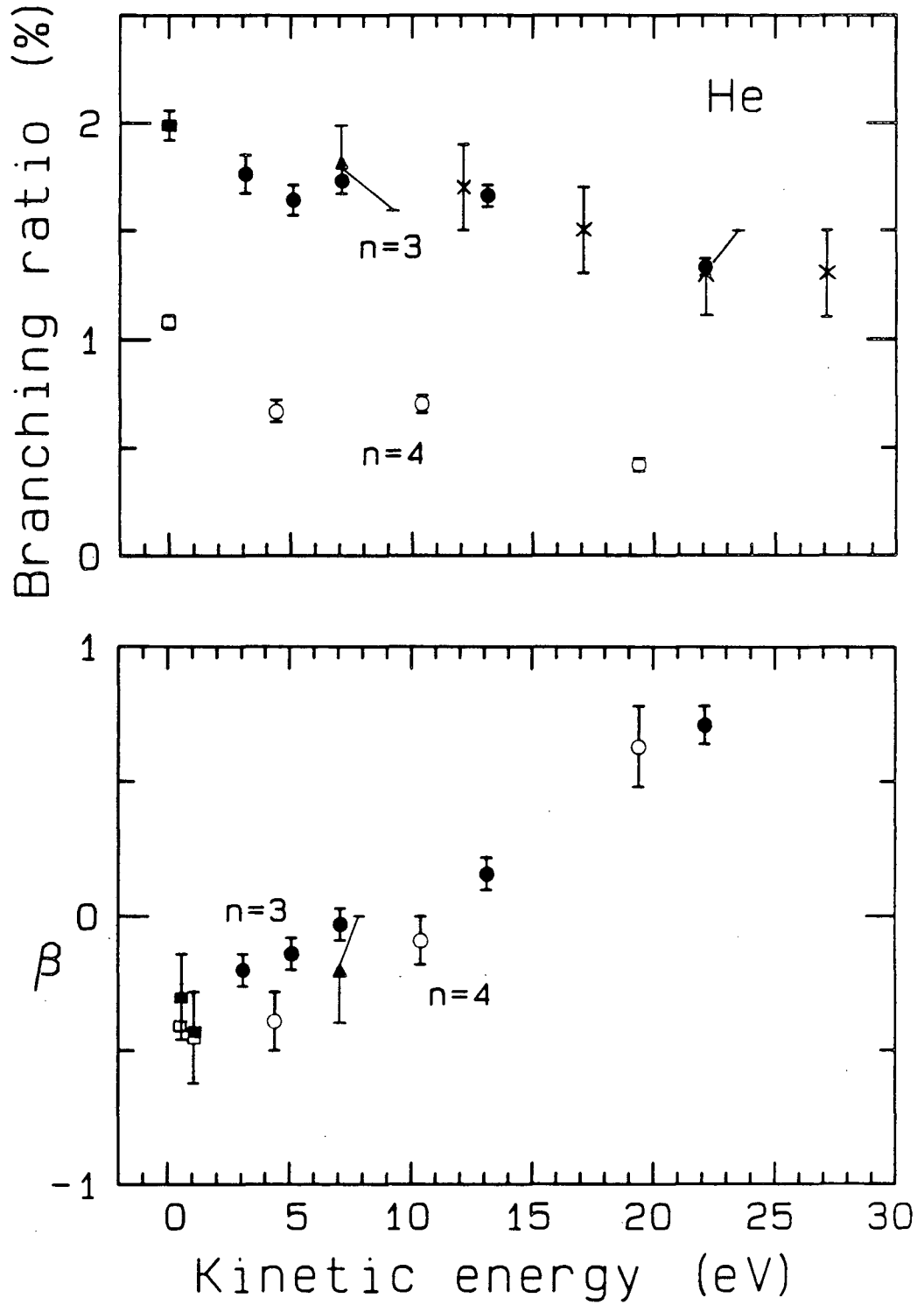
Fig. 1 TOF photoelectron spectrum of He at 80 eV photon energy and with $\theta=54.7^\circ$. The peak label n refers to the principal quantum number of the remaining electron in the He⁺ final state. The small peak to the right of the $n=1$ main line is a result of ringing in the timing circuit, displacing a small fraction of the true counts by a few channels.

Fig. 2 Helium photoelectron satellite branching ratios relative to the $1s$ main-line intensity (top) and asymmetry parameters (bottom) plotted against energy above the satellite thresholds. Solid symbols are for the $n=3$ satellite, open symbols for $n=4$. Circles represent the present results, squares are from Ref. 25, triangles are from Ref. 13, and X's are from Ref. 23. The $n=3,4$ satellite binding energies are 72.9 and 75.6 eV, respectively.²⁹



XBL 852-1070

Figure 1



XBL 867-2806

Figure 2

This report was done with support from the Department of Energy. Any conclusions or opinions expressed in this report represent solely those of the author(s) and not necessarily those of The Regents of the University of California, the Lawrence Berkeley Laboratory or the Department of Energy.

Reference to a company or product name does not imply approval or recommendation of the product by the University of California or the U.S. Department of Energy to the exclusion of others that may be suitable.

*LAWRENCE BERKELEY LABORATORY
TECHNICAL INFORMATION DEPARTMENT
UNIVERSITY OF CALIFORNIA
BERKELEY, CALIFORNIA 94720*